EUROPEAN JOURNAL OF MATERIALS SCIENCE AND ENGINEERING
Volume 11, Issue 3, 2026: 255-270 | www.ejmse.ro | ISSN: 2537-4338

DOI: 10.36868/ejmse.2026.11.03.255

INVESTIGATION OF THE MANUFACTURABILITY, MECHANICAL AND DYNAMIC PERFORMANCE OF ASA/MgAl3Zn1 HYBRID SANDWICH COMPOSITE STRUCTURES

Efe Ekrem MUTLU[1,[0009-0001-1269-9272]] , Çağın BOLAT[1,*,[0000-0002-4356-4696]],
Muhammed Turan ASLAN[1,[0000-0002-9713-4763]]

[1]Samsun University, Faculty of Engineering and Natural Sciences, Department of Mechanical Engineering, Ballıca Campus, 55420, Samsun, Türkiye

Abstract

Through this article, the manufacturing possibility, mechanical response, and dynamic characteristic of dissimilar sandwich composite components created by acrylonitrile styrene acrylate (ASA) polymer and MgAl3Zn1 magnesium alloy were examined in detail. Real-time experimental tests were performed together with numerical efforts to understand the mechanisms. The aim was to attain lightweight, mechanically durable, and easy producable composite laminates. Therefore, ASA thermoplastic and low density MgAl3Zn1 alloy were combined. In this context, two alternative configurations of ASA/MgAl3Zn1/ASA and MgAl3Zn1/ASA/MgAl3Zn1, were fabricated depending on the other production variables. Thermoplastic sections were formed via material extrusion-based additive manufacturing (fused deposition modelling). As for the altering printing factors, filling volume was selected as infill ratios of 20%, 60%, and 100%. Metallic sections were cut to desired shapes by means of wire electrical discharge machining (WEDM), and the related layers were adhered via a strong cyanoacrylate-based binder material. To explore the mechanicak replies, uniaxial tensile, three-point bending, and free vibration behaviors were done experimentally and checked up with ANSYS-assisted simulation solutions. The main findings pointed that the average density, ultimate tensile strength, and rigidity of polymer parts stepped up substantially with rising infill ratio. At 100% infill, calculated the tensile strength reached 43.12 MPa and elastic modulus 2.26 GPa, while at 20% infill these were 25.71 MPa and 1.43 GPa, respectively. For the flexural responses, the maximum stress in the ASA/MgAl3Zn1/ASA structure was approximately 327, 431, and 645 MPa for 20%, 60%, and 100% infill. The MgAl3Zn1/ASA/MgAl3Zn1 sequence displayed superior first natural frequency responses. Further, the obtained difference between real tests and ANSYS evaluations indicated that the proposed simulation approach can reflect accurately the mechanical and vibration responbse of the sandwich engineering components.

Keywords: *acrylate-based polymer, MgAl3Zn1, sandwich design, additive manufacturing, flexural modulus, vibration behavior*

Introduction

Materials science is an interdisciplinary field that investigates the relationships among processing, structure, properties, and performance of a material, optimizing these parameters for specific engineering needs. In sectors such as aerospace, automotive, marine, and defense, achieving both lightness and high strength within the same structure has become a critical requirement [1, 2]. Conventional materials, including metals, polymers, and ceramics, often cannot simultaneously provide high strength, low weight, impact resistance, and environmental stability; consequently, composite structures that combine different materials to achieve superior performance have been developed [3].

*Corresponding author: cagin.bolat@samsun.edu.tr

Composite materials are multi-phase engineering materials formed by combining two or more physically and/or chemically distinct constituents at the macroscopic scale, exhibiting superior properties that the individual constituents do not possess on their own. The matrix phase maintains structural continuity and transfers load to the reinforcement phase, while the reinforcement phase determines the strength and stiffness of the composite. Composites can be classified by matrix type into polymer, metal, and ceramic matrix composites, and by reinforcement geometry into particle-reinforced, fiber-reinforced, laminated, and filled (cellular) composites [4, 5].

Sandwich composite structures are a distinctive structural configuration prominent in engineering applications requiring a high strength-to-weight ratio, consisting of two rigid, high-strength outer face sheets separated by a lightweight core material [6, 7]. The system operates mechanically in a manner similar to an I-beam: the face sheets carry the axial stresses arising from bending moments, while the core material keeps the face sheets apart, increasing the moment of inertia and carrying the shear forces. Nowadays, sandwich panels have become an important component of modern structural engineering, incorporating nanotechnology-enhanced cellular cores and advanced composite face sheets. Balsa wood, polymeric foams (PVC, PET), and honeycomb structures are commonly used core materials, with the selection depending on the operating temperature, moisture level, and required energy absorption capacity [8, 9].

The main damage mechanisms governing the performance of sandwich structures include face-core interfacial delamination/debonding, local buckling (wrinkling) of thin face sheets, local collapse (dimpling) in cellular cores, core shear failure, core crushing, and tensile/compressive failure of the face sheets. Accurate characterization of these damage modes is of critical importance, particularly in safety-priority sectors such as aerospace. Due to the high cost of experimental procedures and dimensional uncertainties, finite element method (FEM)-based numerical simulations (ANSYS, Abaqus, Nastran) are widely employed during design validation; in these models [10, 11].

In the manufacture of sandwich composites, the choice of method is governed by the balance between the mechanical requirements of the design, part complexity, and production volume. Apart from the conventional routes like hand lay-up and spray-up, more automation-based approaches like resin transfer molding (RTM), vacuum-assisted resin transfer molding (VARTM), autoclave-supported curing, 3D printing, and filament-based techniques are also widespreadly tried by different researchers [12]. In recent times, the autoclave-supported systems have become the standard production way in the aeronautics and automotive industries. Contrary to this, the integration of layer-by-layer strategies into the fabrication of sandwich cores has fastly developed in recent years. Also, these technologies come to the forefront as an alternative providing design flexibility, diminished source waste, and the ability to form sophisticated geometries at lower expenditures, in comparison with traditional methods [13]. At this point, hybridizing accumulatedly formed (FDM-based) polymer layers with a metallic alloy offers strong opportunities in terms of both ease of fabrication and mechanical endurance.

As for the critical design factors, one of the most remarkable design variables in hybrid sandwich components is the effectiveness of the interfacial connection among the outer face plates and the core materials. At this point, A relatively poor interfacial bond can cause to unexpected delamination damage with edge compression or bending forces. In addition, this situation significantly limits the load-carrying capacity of the main part bodies. As such, in hybrid-based combinations combining dissimilar raw engineering material families, the correct selection of binder, contact surface preparation, and additional curing states can beseen as highly significant [14]. The limited number of endeavors focusing on polymer-metal hybrid sandwich structures in the scholarly archives can be propounded as one of the principal motivations for this study. Especially, combining ASA, a promising thermoplastic polymer resistant to harsh outdoor conditions and UV beams, with MgAl3Zn1 presents a new examination room for engineering applications that require performance, cost, lightness and environmental durability.

When the scientific reports on the energy sorption and dynamic characteristics of sandwich beams reveal that core geometry and the selection of main constituents play a decisive role. Herein, Tarlochan et al. [15] checked up foam-based and architected cores, emphasizing that inner foams determine high-speed deformation effects more evenly than homogeneous patterns. The team showed that honeycomb-based geometries absorb highly effective impact energy through the face sheets. In another work, Feng et al. [16] dsiclosed that octet-truss lattice structures outclass titanium-based structures.

Parente et al. [17] reported that nanoclay (montmorillonite) reinforcement substantially improves the mechanical performance of sandwich structures; 4% nanoclay content increased compressive strength by 150% and tensile strength by 94%. Kausar et al. [18] reported that Elium resin-based glass fiber reinforced sandwich structures achieved a high flexural strength, surpassing epoxy-based systems, and that short-fiber reinforcement of PVC foam cores. Zaharia et al. [19] showed that, among PLA/PHA sandwich structures produced by FFF, the diamond-celled core exhibited the highest compressive and flexural strength.

Kladovasilakis et al. [20] determined that, in Schwarz diamond TPMS-cored structures, FDM provides higher strength while material jetting printing (MJP) offers higher geometric precision and energy absorption capacity. Le and Goo [21] showed that bio-inspired corrugated-core thermal protection panels designed for hypersonic vehicles achieve approximately 65% mass reduction compared with solid Inconel plates. Chenrayan et al. [22] reported that 10% banana fiber reinforcement in epoxy cores increased flexural strength with ANSYS-experimental agreement. Gong et al. [23] examined the effect of Poisson's ratio on the impact resistance of honeycomb-cored structures, showing that re-entrant (negative Poisson's ratio) structures exhibit the largest back-face displacement. Sefidi and Taghipoor [24] demonstrated that energy absorption capacity in expanded-metal lattice-cored beams and insect-wing/bamboo-inspired hybrid cores, respectively could be increased by 28-33% depending on geometry.

The original contribution of this study stems from the first-ever combined use of ASA polymer and MgAl3Zn1 magnesium alloy within a sandwich composite structure, and the holistic investigation of this hybrid system in terms of both manufacturing and performance. The production of ASA layers via material extrusion (additive manufacturing) integrates additive manufacturing into sandwich design, distinguishing it from conventional composite manufacturing techniques; the bonding of the layers using a low-cost cyanoacrylate-based adhesive constitutes a first application for this material combination in the literature. Another original aspect of the study is the integrated evaluation of three-point bending, tensile, and vibration tests together with finite element analyses, allowing both the static and dynamic behavior of the structure to be examined holistically.

Materials and Methods

The ASA (acrylonitrile styrene acrylate) filament used in this study has a diameter of 1.75 mm and a black color, with a recommended bed temperature of 90-110 °C and nozzle temperature of 245-265 °C according to the manufacturer. It is known that ASA is an amorphous thermoplastic because of the presence of the acrylate phase in its structure. It can exhibit suitable mechanical features similar to ABS along with superior ultraviolet (UV) resistance, low water sorption, and strong chemical replies. Here, these properties provide high dimensional accuracy and better surface roughness of produced parts exposed to aggresive outdoor conditions. At this point, looking at the manufacturer info, it is seen that the average density of ASA filament is 1.05-1.10 g/cm³, the modulus of elasticity is 1.3-2.2 GPa, the ultimate tensile strength is 25-45 MPa, and the operating temperature range is -20 to 80 °C.

Al-Zn-based Mg alloy plates was procured by Sarp Aluminum Industry Ltd. Co. (Istanbul, Türkiye). The above-mentioned Mg alloy belongs to the Mg-Al-Zn material system and ensures a sensitive balance of low density and moderate mechanical durability. Different from the pure magnesium systems, the integration of aluminum and zinc metals rises mechanical performance and part formability. The yield strength of the alloy used in this study is 160-200 MPa, the elongation is 10-18%, and the hardness is 60-75 HV, with an operating temperature range of -196 to 150 °C. However, due to the moderate corrosion resistance of magnesium alloys, an additional surface protection layer (e.g., anodizing or coating) may be required for long-term outdoor applications.

Combining ASA's high UV and environmental resistance with the stiffness and lightness advantages of MgAl3Zn1 allowed the complementary properties of these two materials to be exploited: the ASA face sheets serve both a lightening and environmental protection function, while MgAl3Zn1 serves as the load-bearing, stiffness-enhancing layer. General properties of the utilized ASA and Mg alloy were shared in Table 1 and Table 2.

Table. 1. Properties of the ASA

Property	**Values**
Density (g/cm³)	1.05 – 1.10
Elastic modulus (GPa)	1.3 – 2.2
Tensile strength (MPa)	25 – 45
Yield strength (MPa)	20 – 35
Elongation (%)	5 – 20
Hardness (HV)	~10 – 20 (polymer)
Coefficient of thermal expansion (µm/m·K)	70 – 100
Thermal conductivity (W/m·K)	0.17 – 0.20
Operating temperature (°C)	-20 to 80
Corrosion resistance	High (UV resistant)
Manufacturing method	FDM (3D printing)
Density/strength ratio	Moderate

Table. 2. Properties of the MgAl3Zn1 alloy

Density (g/cm³)	**1.74 – 1.78**
Elastic modulus (GPa)	40 – 45
Tensile strength (MPa)	220 – 260
Yield strength (MPa)	160 – 200
Elongation (%)	10 – 18
Hardness (HV)	60 – 75
Coefficient of thermal expansion (µm/m·K)	25 – 27
Thermal conductivity (W/m·K)	90 – 100
Operating temperature (°C)	-196 to 150
Corrosion resistance	Moderate (coating may be required)
Manufacturing method	Rolling, casting, machining
Density/strength ratio	Very high (lightweight metal)

The mechanical test geometries of the ASA specimens were designed in accordance with the ASTM D638 Type 4 standard using SolidWorks 2020, converted to .stl format, and imported into the Flashprint 5.0 slicing software. G-codes consisting of 14,510, 43,648, and 16,367 layer steps were generated for 20%, 60%, and 100% infill ratios, respectivel. The specimens were produced on a Flashforge Creator 3 FDM printer with fixed parameters: nozzle temperature 240-265 °C, bed temperature 90-110 °C, print speed 50-100 mm/s, fan speed 100%, material flow 100%, and nozzle diameter 0.4 mm. The MgAl3Zn1 tensile specimens were designed in AutoCAD 2024R and cut by wire electrical discharge machining (WEDM, DK7732B device) using a molybdenum wire electrode. The specimens were then surface-finished with 240, 400, 800, and 1500 grit sandpaper. WEDM was selected because of its high-precision cutting capability, and surface quality is critical since it directly affects bonding performance and stiffness. Table 3 highlights the FDM procoess variables.

Table 3. Layer-by-layer printing variables

Parameter	Values
Nozzle temperature (°C)	240–265
Bed temperature (°C)	90–110
Print speed (mm/s)	50–100
Fan speed (%)	100
Material flow (%)	100
Nozzle diameter (mm)	0.4

The sandwich structures were prepared in two different sequences, ASA/MgAl3Zn1/ASA and MgAl3Zn1/ASA/MgAl3Zn1, with a length of 200 mm, total thickness of 9 mm (approximately 3 mm per layer), and a width of 20 mm. The layers were bonded using an Omex-brand high-viscosity, fast-curing cyanoacrylate (CA)-based adhesive; this adhesive has a specific gravity and a curing time exceeding 30 seconds at 20 °C. This low-cost and rapidly applicable bonding method offers an alternative approach toward practical, industrial-scale production processes. Fig. 1 shows the detailed views of the produced sandwich structures.

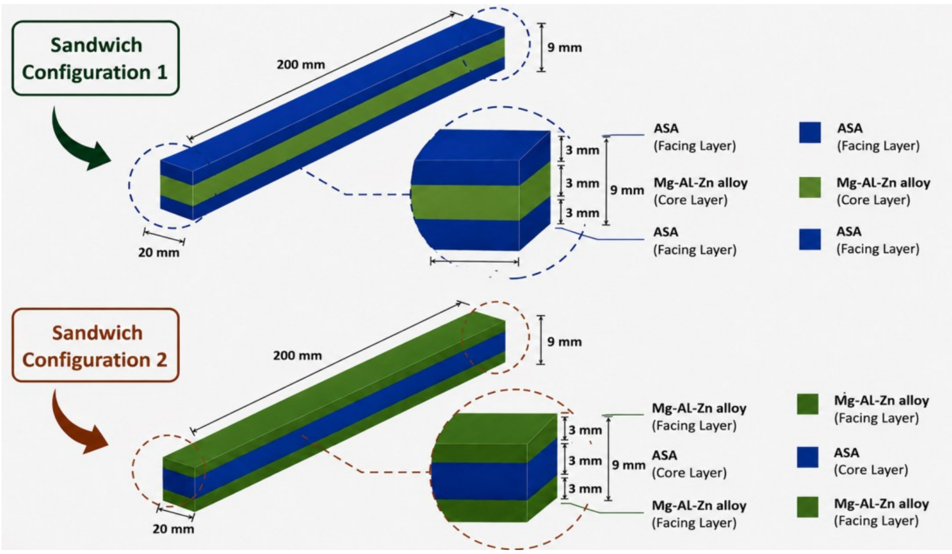

Fig. 1. Schematic of the ASA/MgAl3Zn1 sandwich configurations: Configuration 1 (ASA/MgAl3Zn1/ASA) and Configuration 2 (MgAl3Zn1/ASA/MgAl3Zn1)

Tensile and three-point bending tests were performed using a computer-controlled servo-electromechanical universal testing machine (Besmak BMT300) with a maximum load capacity of 300 kN. All tests were carried out at room temperature and a constant crosshead speed of 5 mm/min. In the vibration tests, the free vibration behavior of beam specimens, clamped at one end over a length of 20 mm with the other end left free, was determined experimentally using a DEWE-43A USB data acquisition system and an accelerometer sensor. As for the numerical studies, all clculations were made in the ANSYS software environment. For the critical material properties like elastic modulus, Poisson's ratio and density were taken from the experimental efforts (uniaxial tensile tests). On the other hand, for the three-point bending analyses, the formed mesh lines at the contact surfaces were compatible and aligned to reach the best convergence limits. Besides, the whole project workflow followed in this study consists of three main stages. Firstly, technical design (creation of CAD models for tensile testing of ASA and MgAl3Zn1) was conducted. Secondly, mechanical testing (axial tensile testing in accordance with ASTM D638 Type 4) procedures were applied. Lastly, finite element analyses (three-point bending, shear testing, and vibration analysis) were realized. That kind of systematic flow ensured that experimental outcomes were utilized directly as numerical model inputs, reducing reliance on generic material databases offered in ANSYS software.

Results and Discussion

Density measurements of ASA beams produced at different infill ratios and taper angles revealed a clear direct proportionality between infill ratio and density, whereas the effect of taper angle on density was found to be quite limited. The highest average density was measured as 1.112 g/cm³ for specimens with 100% infill, while the lowest average density was 0.554 g/cm³ for specimens with 20% infill. In Fig.2, altering density results can be followed.

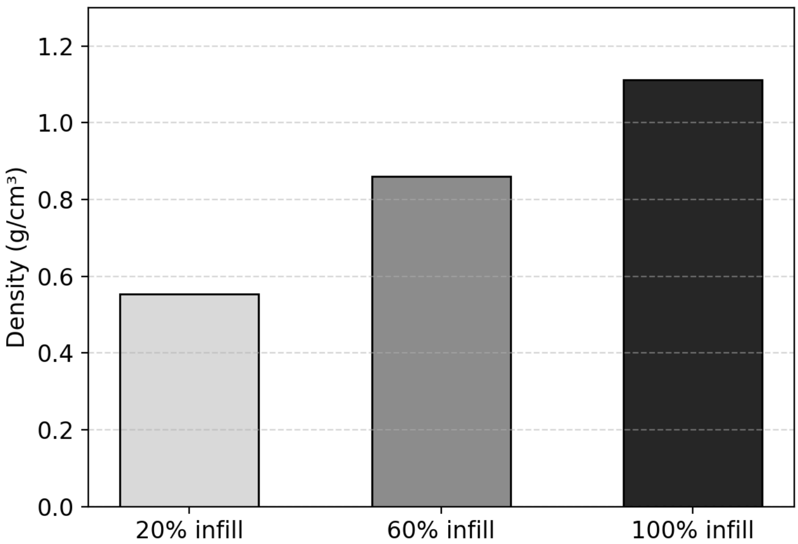

Fig. 2. Relationship between infill ratio and density for the ASA specimens

Tensile tests (Fig. 3) on ASA specimens with different infill ratios showed that specimens with 100% infill exhibited the highest tensile strength (43.12 MPa) and elastic modulus (2.26 GPa), while these values were 25.71 MPa and 1.43 GPa, respectively, for specimens with 20% infill. The increase in the amount of load-bearing material within the structure as the infill ratio increases is responsible for the rise in mechanical strength.

Tensile tests (Fig. 4) conducted on the MgAl3Zn1 magnesium alloy determined an average tensile strength of approximately 266.27 MPa, an elastic modulus in the range of 25.4-26.9 GPa. Also, average density of 1.81 g/cm³ was found fort he metalic parts. These values were used directly as input data in the numerical analyses. The basic mechanical properties of the MgAl3Zn1 magnesium alloy and the ASA polymer used in this study, such as tensile strength, elastic modulus, and density, were not taken from the literature but were obtained directly from the experimental work carried out within the scope of this research.

Six popular deep generative models for polymer design are compared in Table 1, which also highlights the fundamental ideas, structural elements, and working processes of each model. These models capture different facets of polymer structure and generation dynamics, ranging from sequence-based techniques such as Variational Autoencoders (VAEs) and Character RNNs to graph-based models such as GraphINVENT. AAE adds distributional control by adversarial training, ORGAN incorporates domain-specific goals through reinforcement, and VAEs provide smooth latent spaces for interpolation. Each model architecture offers distinct benefits. While REINVENT and CharRNN offer scalable frameworks for sequence-based polymer design using SMILES or p-SMILES representations, graph-based models like GraphINVENT excel at capturing topological subtleties essential to polymer backbones. To help researchers choose the best models for specific generative polymer challenges, associated citations provide additional background information and technical details.

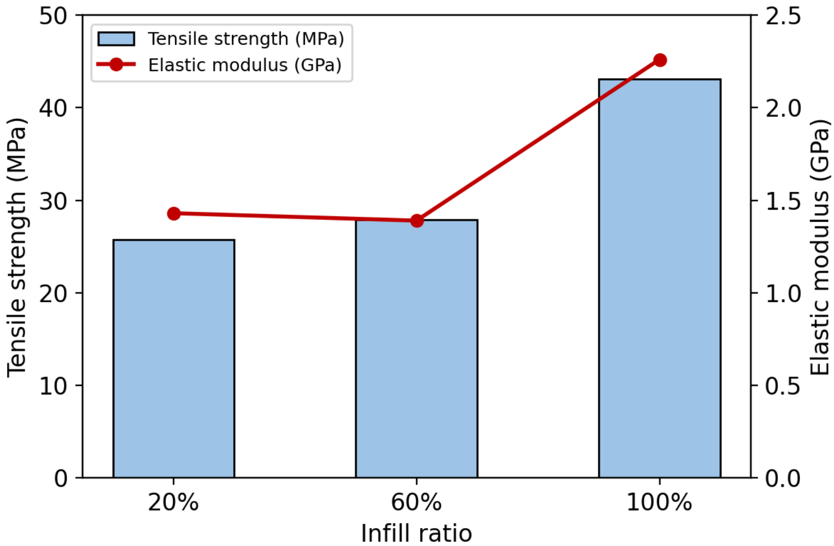

Fig. 3. Tensile strength and elastic modulus of ASA specimens as a function of infill ratio

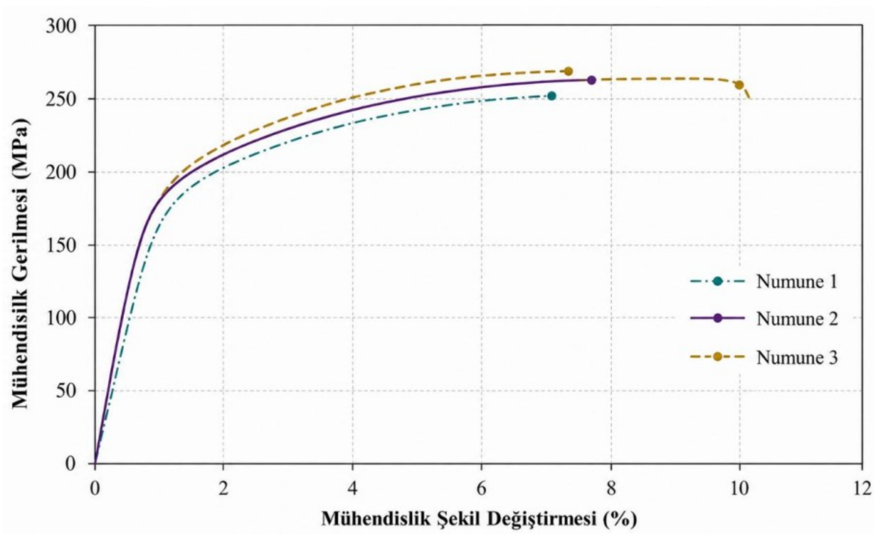

Fig. 4. Engineering stress-engineering strain curves obtained from tensile tests on three replicate MgAl3Zn1 specimens

The collected experiment outcomes were assessed as input variables in the numerical analyses conducted in this study. This methodolgy allows the model to more precisely reflect the real response of the utilized material. As an experimental approach was used in this work, some process factors such as thickness were kept constant, whereas certian significant factors like infill ratio, layer sequence, and taper angle were altered deliberately. Because structural rigidity is a term that directly influences first natural frequency, uniaxial tensile tests were conducted to find the stress-strain curves of the ASA-based layers. Then, these experimental info were added as input factors to the ANSYS analyses, thereby providing more realistic outcomes.

The main interaction between infill ratio and mechanical properties points out that tensile endurence goes up by approximately 68%. Also, elastic modulus rises by 58% as the infill rate escalates from 20% to 100%. This rising-driven characteristic displays a gradual rather than an apparent linear trend, which can be elucidated by the enhancement in interlayer contact area. Load-transfer efficiency also improves as the infill ratio increases in FDM manufacturing. At low infill ratios (20%), the porous internal pattern leads to extra stress concentration places that may cause to premature rupture initiation, whereas at high infill ratios (100%) the polymer part approaches almost a fully dense condition, exhibiting a more homogeneous stress distribution. Overall, these findings put forth that the infill ratio is a factor utterly affecting not only total mass but also the rupture initiation mechanism in the design of extrusion applied polymer components within sandwich structures.

If the practical implications of this paper are evaluated, it can be claimed that the ASA sections obtained by FDM do not serve solely as a ductile filler layer in the sandwich structure. The infill ratio represents an active design variable that allows mechanical performance to be sensitively adjusted. This indicates that, for a fixed geometry and material combination, a family of designs adaptable to different application requirements can be created simply by changing the infill parameter in the slicing software; this is considered one of the most important advantages that additive manufacturing offers to sandwich composite design.

Examination of the natural frequency results for the ASA/Mg/ASA and Mg/ASA/Mg sandwich composite specimens reveals generally high agreement between the ANSYS analyses and the experimental data. In both configurations, the proximity of the numerical results to the experimental values indicates that the developed finite element model successfully represents the free vibration behavior.

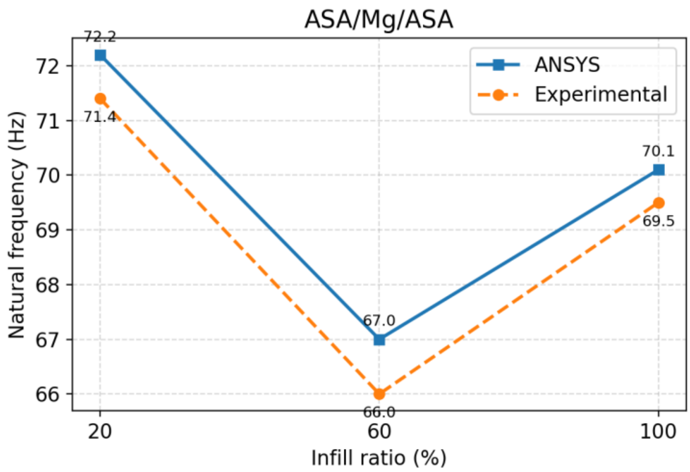

Fig. 5. Natural frequency values of the ASA/Mg/ASA specimen as a function of infill ratio: ANSYS vs. experimental results

For the ASA/Mg/ASA specimens given in Fig. 5, the natural frequency values varied within the range of 66-73 Hz. At 20% infill, the ANSYS result was 72.2 Hz and the experimental result was 71.4 Hz (deviation 0.8 Hz); at 60% infill these values were 67.0 Hz and 66.0 Hz, respectively (deviation 1.0 Hz); and at 100% infill, the ANSYS result was 70.1 Hz and the experimental result was 69.5 Hz, with the deviation reaching its lowest level at 0.6 Hz. In this specimen, the calculated first natural frequency values dropped as long as the filling rate changed from 20% to 60%, then went up again at a full level of 100%. This behavior can be attributed to the altering balance between rigidity and average weight as a function of infill ratio. At 60% infill, the dominance of total weight over average stiffness increase causes the natural frequency to decline, whereas at 100% infill the improved structural stability boosts the frequency.

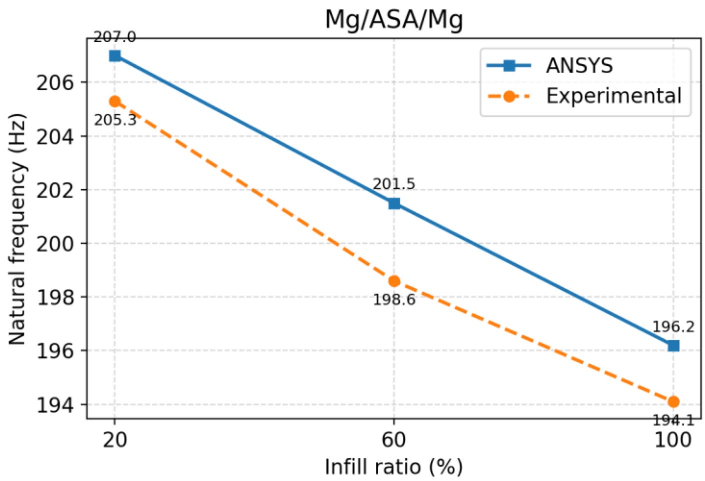

Fig. 6. Natural frequency values of the Mg/ASA/Mg specimen as a function of infill ratio: ANSYS vs. experimental results

When the Mg/ASA/Mg-configured specimen demonstrated in Fig. 6 is assessed, the average natural frequency values ranged from 194 to 207 Hz. This interval is significantly higher than those of the ASA/Mg/ASA-configured specimen. The observation between the two configurations can be accounted for the positioning of the magnesium sections on the outer faces. In sandwich composites, the face parts have a major impact on flexural stiffness, so placing the rigid metal plates on the outside escalated the dynamic stiffness of the composite and augmented the first natural frequency levels. By way of this stacking sequence, the deviations for 20%, 60%, and 100% filling rates were found as 1.7 Hz, 2.9 Hz, and 2.1 Hz, respectively. The gradual decrement in vibration frequency with rising filling rates can be associated with the weigth growth in the polymer core that converts more dominant compared to the total flexural modulus increment.

Considering the all configurations, the ANSYS predictions being somewhat more than the measured experimental outcomes can be as an expected situation. This is because, in the numerical model, the major constituents are typically assumed to be homogeneous, isotropic, and flawless. On the other side, the real test samples may contain gaps/porosities stemming from layer-by-layer fabrication, thickness changes in the binder layer, and interfacial contact problems. Nevertheless, the low magnitude of the deviation values indicates that the numerical model used is reliable. In conclusion, layer sequence was found to have a significant effect on natural frequency. The Mg/ASA/Mg configuration exhibited higher natural frequency values than the ASA/Mg/ASA structure due to the positioning of the magnesium layers on the outer surfaces. Therefore, the Mg/ASA/Mg sequence can be considered a more advantageous design alternative for lightweight structural applications requiring high stiffness and dynamic stability.

3-point bending tests were used to evaluate the load-carrying capacity, deformation behavior, and stiffness variations of the specimens; in addition, ANSYS analyses were used to numerically examine the stress distributions. In this way, the effects of infill ratio and material sequence on the mechanical performance of sandwich composites were comparatively presented. Fort he numerical evaluations, detailed mesh structures were created both fort he tested samples and tester rollers to provide better contact surfaces. Fig. 7 indicates the systematic mesh networks.

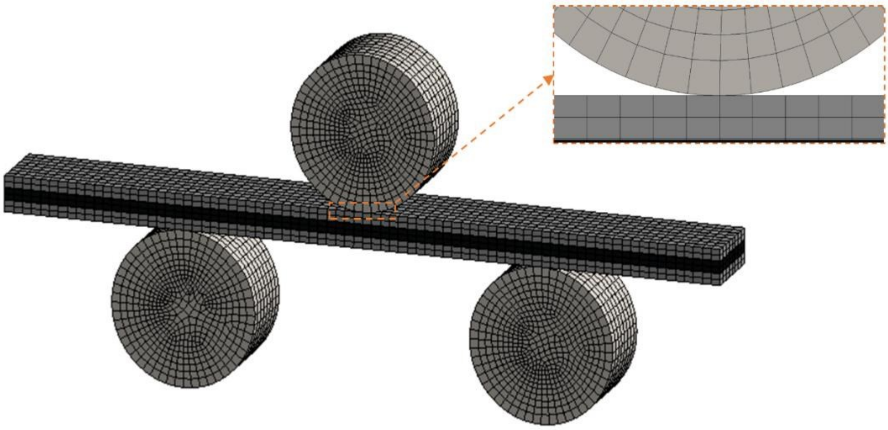

Fig. 7. Mesh configuration used in the three-point bending finite element analysis

Examination of the three-point bending results for the ASA-MgAl3Zn1-ASA sandwich composites shows that bending strength and stiffness increase significantly as the MgAl3Zn1 infill ratio increases. At 20% infill, the stress level was lower, with a maximum stress of approximately 327 MPa; at 60% infill, this value rose to approximately 431 MPa, and at 100% infill it reached its highest level of approximately 645 MPa. In the ANSYS visualizations shown in Fig. 8, stresses were concentrated particularly in the central loading region and on the lower surface; this is a natural result of the three-point bending test, where the upper region experiences compressive stress and the lower region experiences tensile stress. The real test findings and ANSYS curves illustrated in Fig. 9 reflects similar trends to a large extent, pointing that as long as the infill ratio ascends up to the full level, the proposed sandwich structure can withstand against more force levels, even though the recorded nomimal stress concentrations are detected more pronounced, particularly in the central regions.

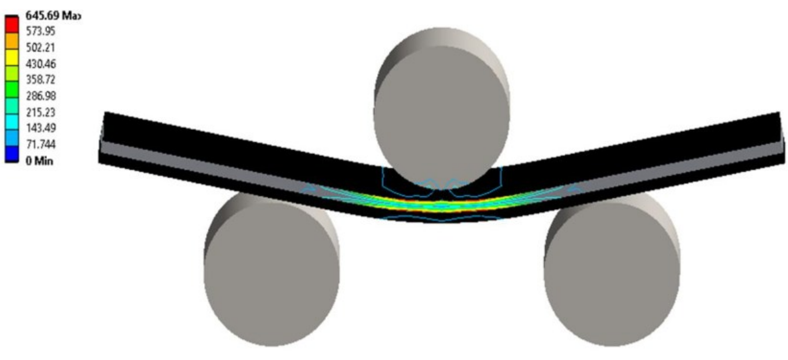

Fig. 8. ANSYS stress contour for the ASA-MgAl3Zn1-ASA specimen at 100% infill under three-point bending

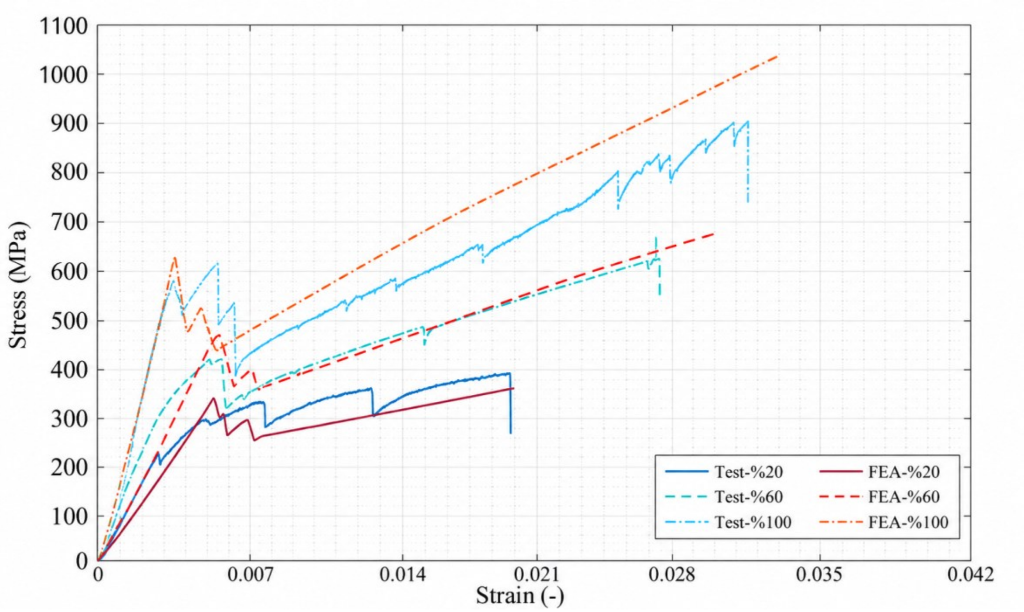

Fig. 9. Experimental (Test) and theoretical/numerical (FEM) stress-strain curves for the ASA-MgAl3Zn1-ASA sandwich specimens at 20%, 60%, and 100% infill

In the Mg dominant test samples, calculated nominal stresses under three-point bending were detected to accumulate especially in the force application zone and near the lower support points given in Fig. 10. The utilization of Mg layers on the face plates strengthened the average flexural stiffness of the sandwich and affirmatively affected its force resistance ability.

When the lowest filling rate (20 %) was glanced at, it is correct to say that the stress distribution remained almost limited due to the fact that the structure shows a tendency toward earlier deformation. Afterwards, at 60% infill, the nominal stresses were distributed more evenly which results in strong agreement between the experimental and ANSYS outcomes. For 100% infill, the highest nominal stress value stepped up notably, with high stress concentrations occurring in the central zone. These findings confirm that as the infill ratio increases, the material becomes stiffer and capable of withstanding higher bending loads (Fig. 11).

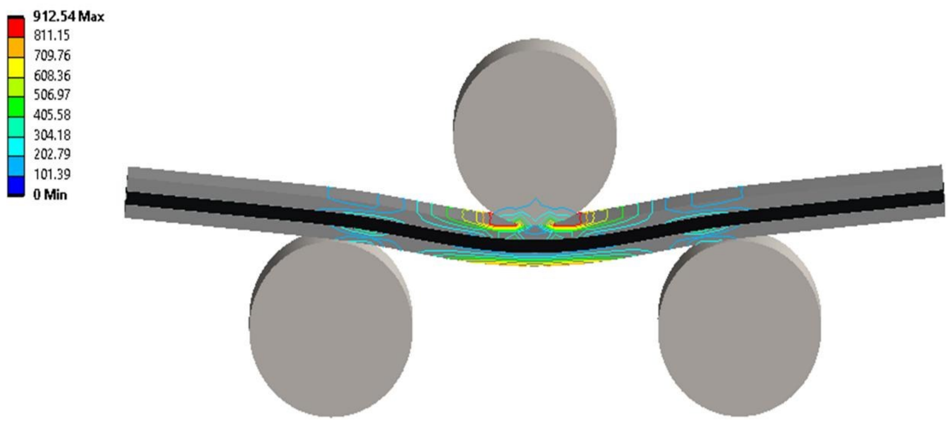

Fig. 10. ANSYS stress contour for the MgAl3Zn1-ASA-MgAl3Zn1 specimen at 100% infill under three-point bending

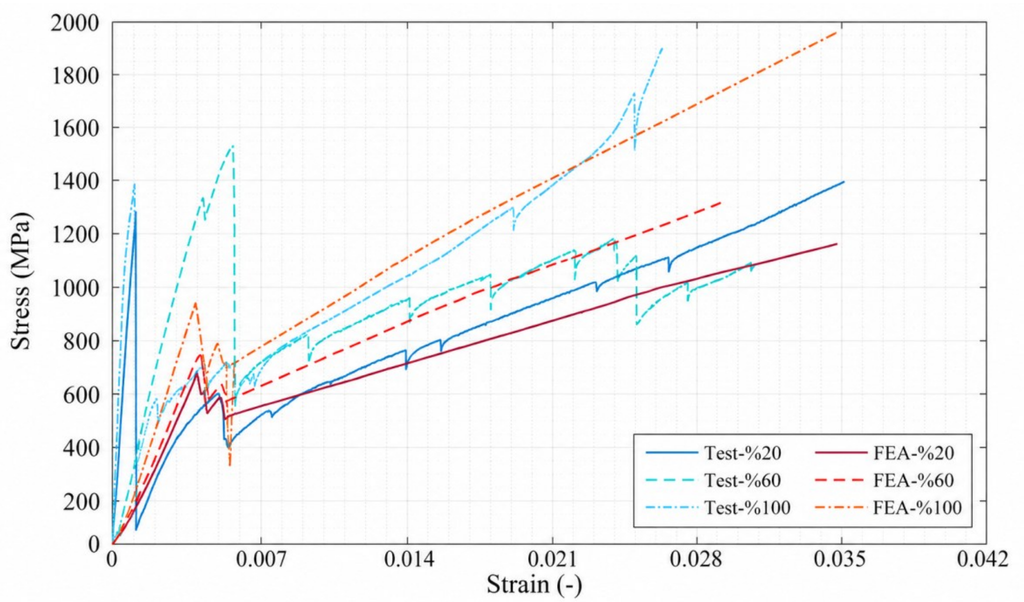

Fig. 11. Experimental (Test) and theoretical/numerical (FEM) stress-strain curves for the MgAl3Zn1-ASA-MgAl3Zn1 sandwich specimens at 20%, 60%, and 100% infill

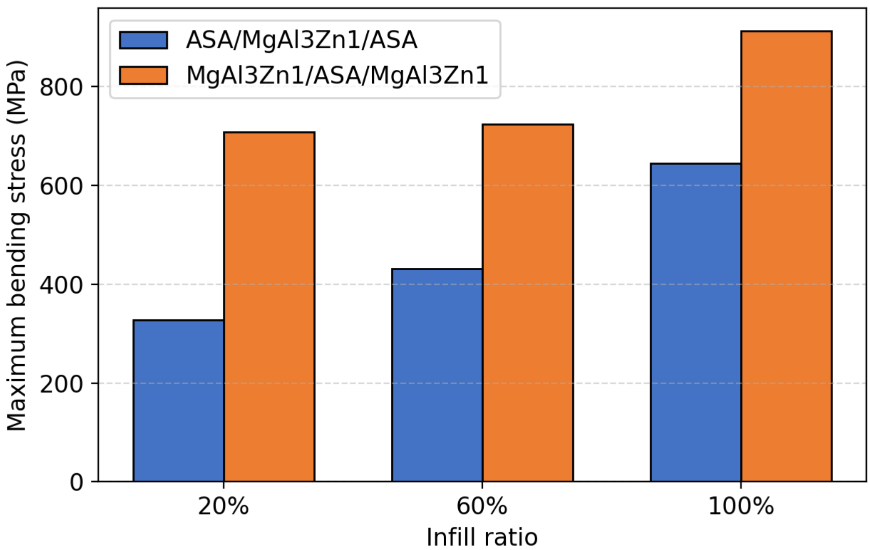

Fig. 12. Comparison of maximum bending stress between the two sandwich configurations as a function of infill ratio.

Comparing the two configurations, the MgAl3Zn1-ASA-MgAl3Zn1 sequence reached markedly higher bending stress values than the ASA-MgAl3Zn1-ASA sequence; for example, at 100% infill the experimental peak stress reached approximately 912 MPa for the MgAl3Zn1-ASA-MgAl3Zn1 structure, while it remained at approximately 645 MPa for the ASA-MgAl3Zn1-ASA structure (Fig. 12). This difference arises because the presence of metallic layers with a higher elastic modulus on the outer surfaces substantially increases the axial-stress-carrying capacity of the face sheets under bending load; this observation is also theoretically supported by sandwich beam theory, in which bending stiffness is proportional to the product of the face-sheet elastic modulus and the square of the distance of the face sheet from the neutral axis. Nevertheless, the sudden drops observed in the experimental curves of both configurations (sharp stress losses following stress build-up) indicate progressive delamination occurring at the adhesive interface, a phenomenon not fully captured by the numerical model, since the interface was defined as an ideal bond in the ANSYS model and progressive damage modeling was beyond the scope of this study.

The fractures observed in both the ASA-Mg-ASA and Mg-ASA-Mg sandwich composite specimens during the three-point bending tests can be attributed to the interfacial bonding quality between the layers and to the manufacturing conditions. The stiffness mismatch between Mg and ASA causes the two layers to deform at different rates under loading, generating stress concentrations at the interfacial regions. In particular, insufficient cleaning or roughening of the bonding surface, or failure to remove the oxide layer on the magnesium surface, can reduce bond strength and increase the risk of delamination. In addition, non-uniform adhesive thickness, with some regions containing excess or insufficient adhesive and resulting voids between the materials, can create weak points for crack initiation and propagation. Considering the major effects of flexural loads, that kinds of defects can move swiftly, causing to interlayer delamination, local ruptures, and brittle fracture. According to this, it can be put forth that the monitored failure emerges not only from material strength but also from interfacial condition and binder material quality.

The mechanical and vibrational observations attained also allow for an assessment of the probable implementation areas of the ASA/MgAl3Zn1 hybrid composites. The low density of the composite resulting from the low density of ASA (1.05-1.10 g/cm³) enables a significant total mass advantage over standard fully metallic structures. Herein, this important feature can be benefited in applications such as portable equipment enclosures, lightweight structural panels, and low-load-bearing support elements. Aside from the literature materials such as shape memory composites, composite foams and cellular structures [25, 26, 27], sandwich combinations have a great potential for aviation, marine, defense, construction, outdoor, and automotive industries. The UV and environmental resistance of ASA supports the usability of the structure in components exposed to outdoor conditions (e.g., façade panels, vehicle body accessories, or lightweight design elements). On the other hand, the high natural frequency values offered by the MgAl3Zn1/ASA/MgAl3Zn1 sequence indicate that this configuration could be preferred in vibration-sensitive lightweight structural applications (e.g., non-load-bearing equipment supports or components requiring vibration isolation). In addition, the high bending stress values obtained for the MgAl3Zn1-ASA-MgAl3Zn1 configuration (an experimental peak value of approximately 912 MPa at 100% infill) indicate that this sequence could also be considered for applications requiring high static load-carrying capacity. However, given the observed interface-related damage mechanisms, before these hybrid structures can be directly integrated into applications requiring high safety levels (such as primary aerospace structural elements), the bonding process needs to be standardized at an industrial scale and supported by long-term durability testing.

Conclusion

In this study, the mechanical and dynamic behavior of hybrid sandwich composite structures combining ASA polymer and MgAl3Zn1 magnesium alloy was investigated experimentally and numerically. Sandwich composite parts were prepared in two different layer stacking sequences: ASA-MgAl3Zn1-ASA and MgAl3Zn1-ASA-MgAl3Zn1. ASA sections were created at 20%, 60%, and 100% infill ratios by means of FDM-based additive manufacturing. The results indicates that filling rate and stacking layer configuration possess an obvious influence on the final performance of the composites.

From the average density levels and uniaxial tensile deformation results, the part density, ultimate tensile strength, and elastic modulus of the polimer samples escalated together with rising infill ratio. Besides, the specimens at 100% infill reflected the highest mechanical responses. However, when weight and stress distribution were evaluated together, rather than maximum strength alone, the 60% infill ratio was found to provide a more balanced structure. The flexural deformation tests also indicated that bending resistance improved with rising infill ratio. However, nominal stress concentrations in the force application zone became more evident at 100% infill rates. In the natural frequency examinations, the configuration in which the Mg layers were put on the outer faces was detected to provide higher natural frequency values. The related findings imply that positioning the Mg layers on the face surfaces heighten flexural stiffness and enhances the dynamic response of the sandwich composites. The apparent agreement between the numerical analysis and the real test data makes a sign that the developed finite element approach can reflect the behavior of the sandwich structure in a large scale. Indeed, ASA/MgAl3Zn1-oriented hybrid laminates are seen as a suitable alternative in terms of low mass, stiffness, and formability. For the next efforts, it is suggested that effective surface preparation operations and binder metarial types can be tested to improve interfacial bonding quality. In the ANSYS analysis, more detailed definition of the adhesive layer and damage progression could yield anticipations closer to the real test results.

This paper show that polymer-metal hybrid sandwich parts are not only an scientific curiosity within the context of lightweight structural engineering, but that practical and scalable engineering solutions can be created by combining additive manufacturing with traditional metal processing methods. Especially, the acceptable mechanical performance achieved using a low-cost bonding method suggests that such hybrid structures could serve as a fast and economical alternative for prototyping and small- to medium-scale production scenarios.

Credit authorship contribution statement

Efe Ekrem Mutlu: Conceptualization, Methodology, Software, Original draft writing, Investigation, Data curation. Muhammed Turan Aslan.: Mechanical tests, Data curation, Methodology. Çağın Bolat: Conceptualizm, Methodology, Data evaluation, Editing, Supervising.

Acknowledgments

As authors, we would like to thank to the supplier firms mentioned in the text for their rapid delivery of polymeric and metallic raw materials.

References

[1] H. Z. Hassan and N. M. Saeed, "Advancements and applications of lightweight structures: A comprehensive review," *Discover Civil Engineering*, vol. 1, no. 1, p. 47, 2024.
[2] Ç. Bolat and A. Gökşenli, "Fabrication optimization of Al 7075/Expanded glass syntactic foam by cold chamber die casting," *Archives of Foundry Engineering*, vol. 20, no. 3, 2020.
[3] P. K. Anthony, "Advanced composite materials for aerospace applications," *Research Output Journal of Engineering and Scientific Research*, vol. 3, no. 2, pp. 1-4, 2024.
[4] İ. C. Akgün, Ç. Bolat, and A. Gökşenli, "Compression properties of cost-efficient porous expanded clay reinforced AA7075 syntactic foams fabricated by industrial-oriented die casting technology," *China Foundry*, vol. 21, no. 1, pp. 60-70, 2024.
[5] Y. Karabulut and R. Ünal, "Additive manufacturing of ceramic particle-reinforced aluminum-based metal matrix composites: A review," *Journal of Materials Science*, vol. 57, no. 41, pp. 19212-19242, 2022.

[6] B. Yıldız, B. Ergene, Ç. Bolat, and H. Ispartalı, "A comparative study on the influence of stacking sequence, infill ratio, and infill pattern on the impact performance of functionally layered PLA and PETG fabricated by additive manufacturing," *Polymers for Advanced Technologies*, vol. 37, no. 2, Art. no. e70491, 2026.
[7] A. Kausar, I. Ahmad, S. A. Rakha, M. H. Eisa, and A. Diallo, "State-of-the-art of sandwich composite structures: Manufacturing-to-high performance applications," *Journal of Composites Science*, vol. 7, no. 3, p. 102, 2023.
[8] J. Pach, R. Wróblewski, and B. Muszyński, "Comparative analysis of sandwich composites with Balsa, Rohacell®, and Nomex® cores for aerospace applications," *Materials*, vol. 18, no. 5, p. 1126, 2025.
[9] A. Rajput, M. R. Sunny, and A. Sarkar, "Optimization of honeycomb parameters of sandwich composites for energy and specific energy absorption using particle swarm optimization," *Marine Structures*, vol. 92, Art. no. 103498, 2023.
[10] M. Kumar, V. R. Kar, and M. L. Chandravanshi, "Free vibration analysis of sandwich composite plate with honeycomb core," *Materials Today: Proceedings*, vol. 56, pp. 931-935, 2022.
[11] A. Kumar, S. Angra, and A. K. Chanda, "Analysis of effect of variation of honeycomb core cell size and sandwich panel width on the stiffness of a sandwich structure," *Research on Engineering Structures & Materials*, vol. 8, no. 1, pp. 45-56, 2022.
[12] J. Wu and Y. Gao, "High-performance electromagnetic shielding composite materials based on carbon nanotubes and sandwich laminate structures," *Polymer Composites*, vol. 45, no. 15, pp. 13639-13649, 2024.
[13] Ç. Bolat, M. T. Aslan, A. Çebi, T. E. Gene, and H. Ispartalı, "A comprehensive analysis of the influence of adhesive types and layer stacking sequence on tensile and impact responses of ASA/PLA composite sandwich structures by additive manufacturing," *Journal of Polymer Research*, vol. 32, no. 5, p. 174, 2025.
[14] M. K. TS, S. Joladarashi, and S. M. Kulkarni, "Comprehensive review of modeling and material selection for hybrid sandwich composites for ballistic impact application using Six Sigma DMAIC methodology," *Proceedings of the Institution of Mechanical Engineers, Part C: Journal of Mechanical Engineering Science*, vol. 239, no. 10, pp. 3703-3724, 2025.
[15] F. Tarlochan, "Sandwich structures for energy absorption applications: A review," *Materials*, vol. 14, no. 16, p. 4731, 2021.
[16] Y. Feng, H. Qiu, Y. Gao, H. Zheng, and J. Tan, "Creative design for sandwich structures: A review," *International Journal of Advanced Robotic Systems*, vol. 17, no. 3, pp. 1-24, 2020.
[17] J. Parente, P. N. B. Reis, M. Neto, and A. M. Amaro, "Mechanical properties of sandwich composites reinforced by nanoclays: An overview," *Applied Sciences*, vol. 10, no. 7, p. 2637, 2020.
[18] A. Kausar, I. Ahmad, S. A. Rakha, M. H. Eisa, and A. Diallo, "State-of-the-art of sandwich composite structures: Manufacturing-to-high performance applications," *Journal of Composites Science*, vol. 7, no. 3, p. 102, 2023.
[19] S. M. Zaharia, L. A. Enescu, and M. A. Pop, "Mechanical performances of lightweight sandwich structures produced by material extrusion-based additive manufacturing," *Polymers*, vol. 12, no. 8, p. 1740, 2020.
[20] N. Kladovasilakis, P. Charalampous, K. Tsongas, I. Kostavelis, D. Tzetzis, and D. Tzovaras, "Experimental and computational investigation of lattice sandwich structures constructed by additive manufacturing technologies," *Journal of Manufacturing and Materials Processing,* vol. 5, no. 3, p. 95, 2021.
[21] V. T. Le and N. S. Goo, "Thermomechanical performance of bio-inspired corrugated-core sandwich structure for a thermal protection system panel," *Applied Sciences*, vol. 9, no. 24, p. 5541, 2019.

[22] V. Chenrayan, G. Gebremaryam, K. Shahapurkar, K. Mani, Y. Fouad, M. A. Kalam, N. M. Mubarak, M. E. M. Soudagar, and B. S. Abusahmin, "Experimental and numerical assessment of the flexural response of banana fiber sandwich epoxy composite," *Scientific Reports*, vol. 13, Art. no. 18156, 2023.
[23] X. Gong, C. Ren, Y. Liu, J. Sun, and F. Xie, "Impact response of the honeycomb sandwich structure with different Poisson's ratios," *Materials*, vol. 15, no. 19, p. 6982, 2022.
[24] M. Sefidi and H. Taghipoor, "Analysis of deformation and failure mechanism of sandwich beams with lattice core under three-point bending load," *Scientific Reports*, vol. 14, Art. no. 13302, 2024.
[25] Ç. Bolat, B. Ergene, İ. C. Akgün, U. Karakılınç, and A. Gökşenli, "An experimental examination of the dry drilling machinability features of cellular glass-filled new-generation metallic composite foams," *Materialwissenschaft und Werkstofftechnik*, vol. 54, no. 11, pp. 1378-1389, 2023.
[26] A. Nazir, K. M. Abate, A. Kumar, and J. Y. Jeng, "A state-of-the-art review on types, design, optimization, and additive manufacturing of cellular structures," *The International Journal of Advanced Manufacturing Technology*, vol. 104, no. 9, pp. 3489-3510, 2019.
[27] A. Amadi, M. Mohyaldinn, S. Ridha, and V. Ola, "Advancing engineering frontiers with NiTi shape memory alloys: A multifaceted review of properties, fabrication, and application potentials," *Journal of Alloys and Compounds*, vol. 976, Art. no. 173227, 2024.

Received: July 1, 2026
Accepted: August 8, 2026